

PYROMEMS IGNITER BASED ON A TEMPERATURE GRADIENT: CONCEPT, FABRICATION AND CHARACTERIZATION

D.A. de Koninck¹, U. Bley², V. Gass³, D. Briand¹, and N.F. de Rooij¹

¹Institute of Microengineering (IMT), Ecole Polytechnique Fédérale de Lausanne (EPFL),
Lausanne, Switzerland

²RUAG Ammotec GmbH, Fürth, Germany

³RUAG Aerospace, Emmen, Switzerland

Abstract: A pyroMEMS igniter with increased combustion reliability is presented. The igniter consisted of a thin-film platinum Joule heater fabricated on a borosilicate glass substrate. Two different igniter layouts (meandering and annular) and three different binder mass fractions (5, 10 and 20 %) were evaluated. High-speed videos were used to judge the success or failure of the combustion events. Although the ignition success rate was 100 %, the combustion success rate was approximately 87.5 ± 7.1 % for the annular design versus 12.5 ± 7.1 % for the meandering layout. No effect on success rate was observed for the different binder contents tested. Rather, increasing the binder mass fraction increased the combustion duration.

Keywords: Igniter, Micro-Combustion, PyroMEMS, Solid Propellant

INTRODUCTION

Achieving reliable and repeatable combustion is widely regarded as one of the main impediments to widespread use of high energy-density solid propellants as compact energy sources in microsystems [1]. For backside (aft) ignition of the propellant charge, fuel ejection due to build up of high-pressure combustion products at the igniter/propellant interface is the primary cause of inconsistent combustion [2].

In this communication, the concept, fabrication and characterization of an aft pyrotechnic micro-electro-mechanical system (pyroMEMS) igniter with improved combustion reliability will be presented. Specifically, the effect of igniter design and binder mass fraction on the combustion success rate was investigated using high-speed videos of the combustion event. The present igniter layout was found to significantly increase the combustion reliability over a standard meandering heater, whereas higher binder content increased combustion duration.

CONCEPT AND FABRICATION

The present ignition concept sought to prevent propellant ejection by directing the combustion from the periphery of the drop towards its center, thereby allowing the gaseous combustion products to escape unimpeded (see Figure 1).

This was achieved by patterning an annular resistive heater onto a borosilicate glass substrate, thereby focusing the heating along the edge of the propellant. In addition, the width of the igniter was modulated in order to vary the local wire temperature

and create hot spots on the fuel drop.

The igniters were fabricated via lift-off photolithography of a 235 nm-thick platinum film—with a 15 nm tantalum adhesion layer—deposited using an e-beam evaporator. Two different layouts were produced: the above-mentioned “annular” design as well as a simple “meandering” layout (see Figure 2). The line width and line spacing of the meandering igniter were 50 μm , while the wide and narrow sections of the annular heater measured 100 μm and 10 μm , respectively. The spacing between the two circular heating arms was kept constant at 70 μm .

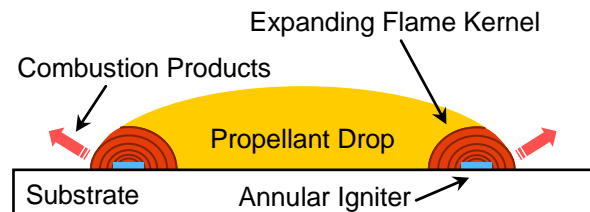


Figure 1: Cross-sectional schematic of the present aft ignition concept to prevent propellant ejection.

The propellant material used in this study was a chemical gas generator that was manually drop-coated onto the igniter to provide good physical and thermal contact between the two. The fuel was custom-prepared to yield a micrometric grain size, thus facilitated deposition via drop-coating. A water-soluble binder was added to the fuel to improve its adhesion with the substrate, thereby further enhancing combustion repeatability. Three different binder mass fractions were tested: 5, 10 and 20 %, yielding a total of 6 treatments across two factors.

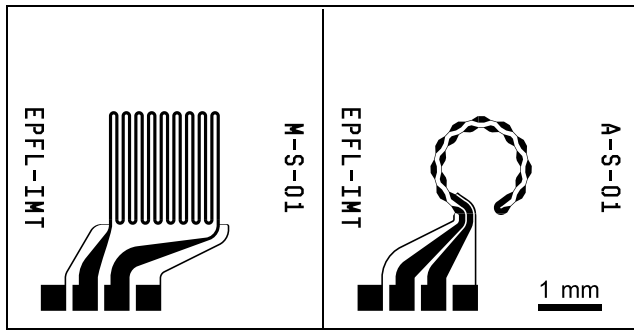


Figure 2: Representative schematics of the meandering- (left) and annular-type (right) pyroMEMS igniter layouts.

EXPERIMENTAL SETUP

A 1-second, square voltage pulse was applied to the igniter chip using a function generator (HP33120A) coupled to a high-speed power amplifier (NF Electronic Instruments 4015). The voltage pulse magnitude was set to generate a 100 mA (nominal) signal through the igniter. Two digital multimeters (Agilent 34411A) measured the voltage and current passing through the igniter during the pulse. Simultaneously, a high-speed framing camera (Photron Ultima APX-RS) acquired images of the combustion process with a resolution of 512 x 544 pixels through a 5x microscope objective. The frame rate was 9000 frames per second with an exposure time of 0.111 ms (i.e., 1/frame rate) to maximize the amount of light received by the CMOS sensor. All of the measurement devices were computer controlled via GPIB connectors using a custom MATLAB script. The function generator was triggered by MATLAB (software trigger), while the multimeters and camera were simultaneously triggered using the transistor-transistor logic (TTL) output of the function generator.

Since the goal of this study was to quantify the effect of igniter design and binder content on the combustion success rate, the fuel-coated igniter chips were chosen so as to minimize the variability in the propellant drop volume and placement on the igniter. A total of 38 chips—19 of each layout type—were selected for this study.

RESULTS AND DISCUSSION

All 38 chips prepared were successfully initiated. The mean input power used to ignite the fuel drop was 2.96 ± 0.17 W for the meandering layout and 1.35 ± 0.04 W for the annular design. No attempt was made to minimize the input power for these tests; rather an arbitrarily large nominal input current was

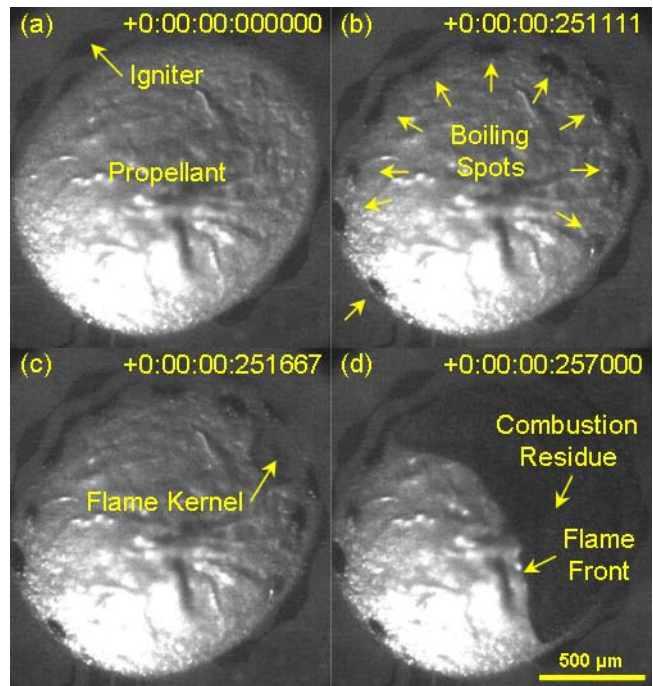


Figure 3: A series of four high-speed video frames of a “successful” combustion (annular layout, 10% binder): (a) before ignition, (b) emergence of boiling spots above narrow sections of igniter, (c) flame kernel ignition, and (d) flame spreading. A time stamp is given in the top right corner of each frame.

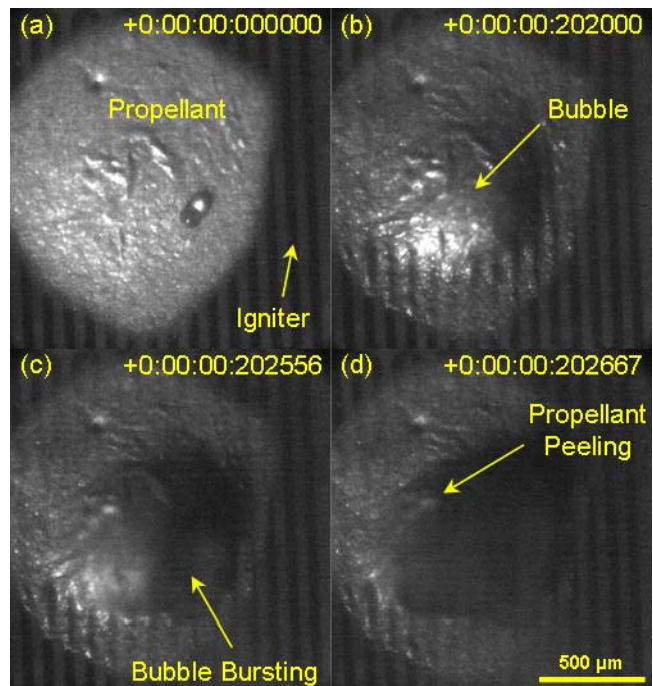


Figure 4: A series of four high-speed video frames of a “failed” combustion (meandering layout, 20% binder): (a) before ignition, (b) bubble formation, (c) bubble rupture, and (d) peeling of drop from substrate. A time stamp is given in the top right corner of each frame.

selected to ensure proper initiation of the fuel. However, using suspended igniters of a similar layout proved to significantly decrease the input power required for ignition [2].

Although the ignition success rate was 100 %, not all the fuel drops burned consistently. A “successful” combustion occurred when the drop remained attached to the substrate throughout the combustion process, as shown in Figure 3. A “failed” combustion was characterized by propellant ejection from the substrate (e.g., Figure 4).

Given the above criteria for assessing a combustion trial success and failure, binomial sampling distributions could be constructed for the different pyroMEMS igniter treatments. The Wilson interval was used to obtain the standard error of the sampling distribution means. It is given as

$$p = \frac{\hat{p} + t/2}{1+t} \pm \frac{\sqrt{\hat{p}\hat{q}t + t^2/4}}{1+t}, \quad (1)$$

where p is the *actual* success rate, \hat{p} and \hat{q} are the *observed* success and failure rates over n trials, $t = (z_{1-\alpha/2})^2/n$ and $z_{1-\alpha/2}$ is the standard normal variable for a two-sided hypothesis test with a level of significance of α . The details of the derivation can be found in [3]; however, it is important to point out that the best estimate for the actual success rate is not the observed success rate \hat{p} , but $(\hat{p} + t/2)/(1+t)$, which converges to the observed success rate for $n \rightarrow \infty$. Also, the Wilson interval always covers the observed success rate no matter the sample size or level of significance. It was used in this study because it provides better coverage of the actual success rate than the standard Wald interval— $\hat{p} \pm \sqrt{\hat{p}\hat{q}t}$ —for small sample sizes and/or extreme probabilities [4]. In addition, two-sample mean difference inferences of all pairwise comparisons were carried out using the Wilson estimate, defined as

$$\left| \left(\frac{\hat{p}_1 + t_1/4}{1+t_1/2} \right) - \left(\frac{\hat{p}_2 + t_2/4}{1+t_2/2} \right) \right| \leq \sqrt{\frac{p_1 q_1 t_1}{1+t_1/2} + \frac{p_2 q_2 t_2}{1+t_2/2}}, \quad (2)$$

where $t_i = (z_{1-\alpha/2})^2/n_i$, $i = \{1, 2\}$. Note: all errors cited in this communication were computed as one standard deviation about the mean (i.e., $z=1$) and all inferences and comparisons were made with a 5 % level of significance (i.e., $z=1.96$).

The annular layout provided a statistically

significant increase in combustion success rate over the meandering design (as shown in Figure 5) with an estimated overall mean success rate of 87.5 ± 7.1 % (17 successes in 19 trials) versus 12.5 ± 7.1 % (2 successes in 19 tests), respectively. Conversely, binder mass fraction had no significant effect on the combustion success rate.

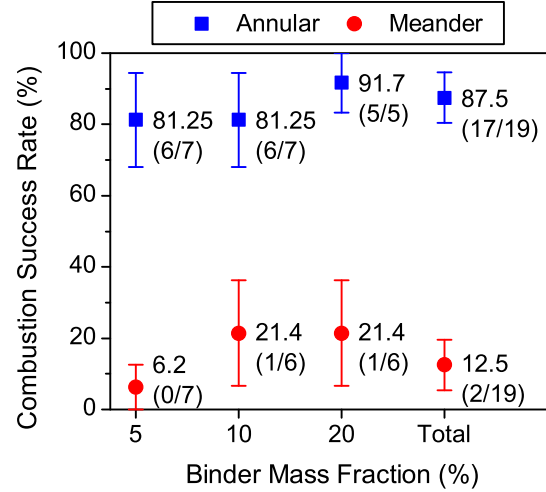


Figure 5: Effect of igniter layout and binder mass fraction on combustion success rate. The error bars represent the standard error of the mean. The numbers in parenthesis are the number of successes (left) and the sample size (right) for the data point.

Comparing the present pyroMEMS igniters with previously published devices (e.g., [5]) is difficult given that previous studies would only report *ignition* success rate, which we have demonstrated to be a poor indicator of combustion reliability.

Beyond providing combustion success/failure data, the high-speed videos also revealed the salient ignition and flame propagation mechanisms for the different igniter treatments. Successful combustion with the annular igniters was always preceded by propellant boiling in the vicinity of the narrow portions of the igniters (Figure 3b). The boiling appeared first where the fuel drop was thinnest—which tended to be along the outer arm of the annular igniter—but could also be found above the inner arm, provided ignition and spreading of the flame kernel did not occur first.

Following a certain induction time, a single flame kernel appeared above one of the “boiling spots” and the combustion front spread outward (Figure 3c). The “apparent flame speed”—as seen from above with the camera—was highly unsteady, such that the flame accelerated in the vicinity of the boiling spots, but decreased in speed over the center of the drop. This resulted in the characteristic sickle-shaped flame front

seen in Figure 3d.

The induction time and combustion duration were estimated from the high-speed videos. The induction time was taken from the time the function generator was triggered (i.e., time zero on video) until a flame kernel first appeared on the surface of the drop. The combustion duration was defined as the time interval between the appearance of the flame kernel and the frame in which no more fuel was consumed. Combustion duration was found to be negatively correlated with induction time, with a mean slope of -0.0423 ± 0.0065 ms/ms (Figure 6). An analysis of covariance found that the effect of binder content was significant. Furthermore, a test of parallel lines found no appreciable difference in the individual slopes. Increasing the binder content from 5 % to 20 % increased the mean combustion duration for the annular igniters by 21.1 ± 5.0 ms. Variations in the combustion time could not be accounted for by differences in the amount of propellant burned (168 ± 22 ng for the successful trials). The amount of propellant consumed was determined by comparing the post-explosion igniter chip mass with that measured before combustion. Therefore, longer induction times allow the fuel drop more time to heat up, thus increasing the flame speed and decreasing the combustion duration. However, it is unclear what mechanisms control the length of the induction time.

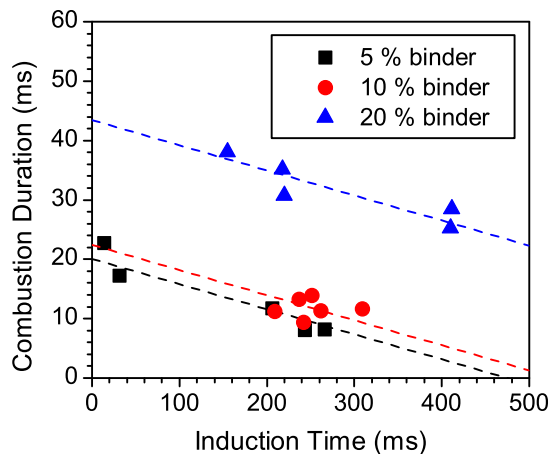


Figure 6: Combustion duration versus induction time for the successful annular trials. Linear best fit curves (dashed lines) obtained from analysis of covariance.

Failed combustion events, on the other hand, occurred due to propellant peeling and ejection. Following the power input, the fuel drop swelled (Figure 4b) and ruptured (Figure 4c), causing the drop to peel away from the substrate (Figure 4d). This behavior is consistent with the build up of high-

pressure gaseous combustion products at the igniter/propellant interface as postulated in ref. [2].

CONCLUSION

High-speed camera filming was shown to be an effective tool in identifying and characterizing the combustion mechanisms in micro-scale solid propellant charges. Ignition success rate was shown to be a poor indicator of combustion reliability. Although both designs yielded flawless ignition success rates, the annular igniter layout proved to be significantly more reliable in producing a stable combustion front than standard meandering-type heaters. Binder mass fraction—within the ranges tested—had no effect on success rate; rather increasing the binder content served to increase the combustion duration.

ACKNOWLEDGEMENTS

The authors are grateful to Prof. A. Fasoli, Dr. I. Furno and particularly Mr. D. Irajii of the EPFL “Centre de Recherches en Physique des Plasmas” for access to and assistance with their high-speed camera. D.A. de Koninck gratefully acknowledges the financial support from the EPFL Space Center ESRP under contract #2007/033 as well as a postgraduate scholarship from the Natural Sciences and Engineering Research Council of Canada (NSERC).

REFERENCES

- [1] Rossi C, Estève D 2005 Micropyrotechnics, a new technology for making energetic microsystems: review and prospective *Sensor Actuat. A-Phys.* **120** 297-310
- [2] Briand D, Guillot L, Bley U, Danninger S, Gass V, de Rooij N F 2008 Digital Micro-Thrusters with Simplified Architecture and Reliable Ignition and Combustion *Technical Digest Power MEMS 2008 (Sendai, Japan, 9-12 November 2008)* 157-160
- [3] Wilson E B 1927 Probable Inference, the Law of Succession, and Statistical Inference *J. Am. Stat. Assoc.* **22** 209-212
- [4] Brown L D, Cai T T, DasGupta A 2001 Interval Estimation for a Binomial Proportion *Stat. Sci.* **16** 101-133
- [5] Rossi C, Briand D, Dumonteuil M, Camps T, Pham P Q, de Rooij N F 2006 Matrix of 10 x 10 addressed solid propellant microthrusters: Review of the technologies *Sensor Actuat. A-Phys.* **126** 241-252